# CONVERGENCE ANALYSIS OF THE ADAPTIVE FINITE ELEMENT METHOD WITH THE RED-GREEN REFINEMENT

XUYING ZHAO, JUN HU, AND ZHONGCI SHI

ABSTRACT. In this paper, we analyze the convergence of the adaptive conforming $P_1$ element method with the red-green refinement. Since the mesh after refining is not nested into the one before, the Galerkin-orthogonality does not hold for this case. To overcome such a difficulty, we prove some quasi-orthogonality instead under some mild condition on the initial mesh (Condition A). Consequently, we show convergence of the adaptive method by establishing the reduction of some total error. To weaken the condition on the initial mesh, we propose a modified red-green refinement and prove the convergence of the associated adaptive method under a much weaker condition on the initial mesh (Condition B).

## 1. INTRODUCTION

The adaptive finite element method (hereafter AFEM) is an efficient and reliable tool in the numerical solution of partial differential equations. The typical structure of the adaptive algorithm is made up of four modules: "Solve", "Estimate", "Mark", and "Refine". For triangular meshes there essentially exist three different local refinement strategies: the longest edge bisection, the newest vertex bisection, and the red-green refinement [26]. The first two refinements are nested refinements while the last is not. Among these refinements, only the complexity of the newest vertex bisection is clear so far [23]. The red-green refinement is in fact, a modification of the usual regular refinement, which is for the purpose of fulfilling local refinement. This refinement was first proposed by Bank[3, 4] and successfully extended to tetrahedron in [18, 20, 11, 15]. Even though adaptivity has been a fundamental tool of engineering and scientific computing for about three decades, the convergence analysis is only recent. It started with Döfler [14], who introduced a crucial marking, from now on called Döfler's marking, and proved the strict energy reduction for the Laplacian provided the initial mesh $\mathcal{T}_0$ satisfies a fineness assumption. By introducing the concept of data oscillation and the interior node property, Morin, Nochetto and Siebert [21, 22] removed restriction on the initial mesh $\mathcal{T}_0$ and proved the convergence of the AFEM. Very recently, Cascon, Kreuzer, Nochetto and Siebert established the convergence of the AFEM without the interior node property for the self-adjoint second order elliptic problem [10]. All of these results are based on an important tool: "Galerkin-orthogonality". There are some works on nonstandard finite element methods in the literature. Carstensen and Hoppe proved the convergence of adaptive nonconforming and mixed finite element methods [9, 8]. One key ingredient of those papers is the so-called "quasi-orthogonality". This technique is extended to the high order mixed finite element methods for the Poisson equation in [12] and the nonconforming $P_1$ finite element method for the Stokes-like problem in [17]. In a very recent paper [16], the second two authors with

*Date*: May 18, 2009.
The second author was supported by the NSFC under Grant 10601003, and A Foundation for the Author of National Excellent Doctoral Dissertation of PR China 200718, and the Scientific Research Foundation for the Returned Overseas Chinese Scholars, State Education Ministry.

their corporator gave unifying convergence analysis of the adaptive Morley-type element methods by adopting the conservative properties of these class of schemes. So far, both Galerkin-orthogonality and quasi-orthogonality can be derived only for the first two refinement strategies where the resulted meshes are nested. There is no work concerning the convergence of the AFEM with the red-green refinement. Since it has been widely used in practical computing, for example, semi-conductor device simulation [26, 18], it is of importance to analyze the convergence of the adaptive algorithm with such a refinement.

The objective of this paper is to study the convergence of the adaptive conforming $P_1$ element method based on the red-green refinement. Since the mesh after refining is not nested into the one before for such a refinement strategy, the Galerkin-orthogonality does not hold for this case. To overcome this difficulty, we prove some quasi-orthogonality which is first proposed for the nonconforming $P_1$ element method [9, 17, 16]. As indicated in [16], the quasi-orthogonality of the Morley-type element methods [9, 16] is the consequence of the conservative properties. Unlike those nonconforming methods, the difficulty herein is not from the nonconformity of the discrete space but from the lack of the nesting of the discrete finite element space. Moreover, no local conservative property can be applied herein. Therefore, one can not expect to derive the quasi-orthogonality as those in [9, 17, 16]. Herein we shall establish a different quasi-orthogonality under some mild assumption on the initial mesh (see Condition A below) and then prove the convergence of the adaptive conforming $P_1$ element method. In addition, we propose a modified red-green refinement and prove the associated adaptive conforming $P_1$ element method under a much weaker condition on the initial mesh(see Condition B below). Note that the Condition B is satisfied by most practical meshes.

The rest of this paper is organized as follows. In the next section, we present the preliminary including the notation, the problem under consideration, and the a posteriori error estimate which is followed by the description of the red-green refinement algorithm. In Section 4, we prove the reduction of the estimator while the quasi-orthogonality appears in Section 5. In Section 6, we prove the main result of this paper, namely the convergence of the adaptive algorithm with the red-green refinement strategy. In Section 7 we give a modified red-green refinement strategy and prove the convergence of the adaptive methods based on it. This paper ends with the conclusion in Section 8.

## 2. Preliminaries

This section presents the necessary notation and the a posteriori error estimate. We assume $\Omega \in \mathbb{R}^2$ to be a bounded, polygonal, open domain with boundary $\Gamma := \partial\Omega$. For a measurable set $G \subset \Omega$, let $(\cdot,\cdot)_G$ and $\|\cdot\|_{0,G}$ denote the inner product and the norm in $L^2(G)$. We also use $(\cdot,\cdot)$ to denote $(\cdot,\cdot)_\Omega$ for simplicity. Furthermore, let $|\cdot|_{m,G}$ and $\|\cdot\|_{m,G}$ denote the seminorm and norm in the Sobolev space $H^m(G)$, respectively. In particular, let $|\cdot|_{1,\Omega}$ stand for the associated seminorm on $H^1(\Omega)$ which actually is a norm on $V := H_0^1(\Omega) := \{v \in H^1(\Omega), v|_\Gamma = 0\}$. Given any nonnegative integer $k$, let $\mathcal{T}_k$ be a triangular partition of the domain $\Omega$ in the sense of [6]. With no risk of confusion, we assume that $\mathcal{T}_{k+1}$ is a refinement of the coarser mesh $\mathcal{T}_k$. Let $\mathcal{E}_k$ be the set of all internal edges of the mesh $\mathcal{T}_k$. Given any interior edge $E$, we denote by $\omega_E := T_1 \cup T_2$ with $T_1 \cap T_2 = E$. For a triangle $T$ with three edges $E_1$, $E_2$, and $E_3$, let $\omega_T := \omega_{E_1} \cup \omega_{E_2} \cup \omega_{E_3}$. Let $V_k \subset V$ be the usual conforming $P_1$ finite element space over the triangulation $\mathcal{T}_k$.

We consider the following second order elliptic equation

$$\begin{cases} -\mathrm{div}(\mathbf{A}\nabla u) = f & \text{in} \quad \Omega, \\ u = 0 & \text{on} \quad \partial\Omega. \end{cases} \tag{2.1}$$

where $f \in L^2(\Omega)$ and $\mathbf{A}$ is positive and piecewise constant. We assume that $\mathbf{A}$ is constant on each triangle of the initial mesh $\mathcal{T}_0$.

The weak formulation of the problem (2.1) reads: Find $u \in V$ such that

$$a(u,v) = (f,v), \quad \forall\ v \in V, \tag{2.2}$$

where the bilinear forms $a(u,v) = \int_\Omega \mathbf{A}\nabla u \cdot \nabla v\ dx$ and $(f,v) = \int_\Omega fv\ dx$. Given $S \subset \Omega$, we denote by $|||u|||_S$ the energy norm $\|\mathbf{A}^{\frac{1}{2}}\nabla u\|_{0,S}$. Obviously, for any $u \in V$, $|u|_{1,\Omega}$ and $|||u|||$ are two equivalent norms, i.e.,

$$c_a\ |||\ u||| \le |u|_{1,\Omega} \le C_a\ |||\ u|||\ . \tag{2.3}$$

The discrete weak formulation of the problem (2.1) reads: Find $u_k \in V_k$ such that

$$a(u_k, v_k) = (f, v_k), \quad \forall\ v_k \in V_k. \tag{2.4}$$

We end this section by presenting the a posteriori error estimate from, for instance, [1, 26]. Denote $W_{\mathcal{T}_k} := \{w \in H^1(\Omega) \mid w \text{ is a piecewise linear function on } T, \forall T \in \mathcal{T}_k\}$. Obviously, $V_k \subset W_{\mathcal{T}_k}$. Given any interior edge $E$, we define the edge jump function[①]

$$J(v)|_E := (\llbracket \mathbf{A}\nabla v \rrbracket \cdot \overrightarrow{n_E})|_E := (\mathbf{A}\nabla v|_{T_1}) \cdot \overrightarrow{n_E} - (\mathbf{A}\nabla v|_{T_2}) \cdot \overrightarrow{n_E}, \quad \forall v \in H_0^1(\Omega) \cap W_{\mathcal{T}_k}.$$

with the unit outer normal $\overrightarrow{n_E}$ of $E \subset \partial T_1$. Given $T \in \mathcal{T}_k$, we define the local estimator as

$$\eta_k^2(v,T) := h_T^2 \|\ f\ \|_{0,T}^2 + h_T \|\ J(v)\ \|_{0,\partial T \cap \Omega}^2, \quad \forall v \in H_0^1(\Omega) \cap W_{\mathcal{T}_k},$$

where $h_T := |T|^{\frac{1}{2}}$. For any subset $\mathcal{T}_k' \subset \mathcal{T}_k$, we define $\eta_k^2(v, \mathcal{T}_k') := \sum\limits_{T \in \mathcal{T}_k'} \eta_k^2(v,T)$. For the case where $\mathcal{T}_k' = \mathcal{T}_k$ and $v = u_k$, we use $\eta_k$ to denote $\eta_k(u_k, \mathcal{T}_k)$ for short. For this estimator, one has the following reliability and efficiency.

**Lemma 2.1** (reliability and efficiency)**.** *Let $u \in V$ and $u_k \in V_k$ be the solutions of problems (2.2) and (2.4), respectively. It holds*

$$|||u - u_k|||^2 \le C_1 \eta_k^2, \tag{2.5}$$

$$C_2 \eta_k^2 \le |||u - u_k\ |||^2 + osc^2(f, \mathcal{T}_k), \tag{2.6}$$

*where the oscillation $osc(f, \mathcal{T}_k) = \left( \sum\limits_{T \in \mathcal{T}_k} \|h_T(f - f_T)\|_{0,T}^2 \right)^{\frac{1}{2}}$ and the average $f_T = \frac{\int_T f\ dx}{|T|}$.*

The analysis in the sequel is based on the following assumption on the initial mesh $\mathcal{T}_0$:
Condition A: Given $T \in \mathcal{T}_0$, let $a_1, a_2$ and $a_3$ be its three edges with the corresponding heights $h_1, h_2$ and $h_3$, respectively. Assume that

$$|h_i| > 1/2|a_i| \quad \text{or} \quad |T| > 1/4|a_i|^2, \quad i = 1,2,3\ ,$$

where $|\cdot|$ denotes the length or the area.

Let $\rho(T) = \max\{\frac{a_1}{2h_1}, \frac{a_2}{2h_2}, \frac{a_3}{2h_3}\}$. Condition A implies $0 < \rho(T) < 1$.

**Remark 2.2.** *One sufficient condition for Condition A is as follows: Each angle of $T$ is larger than $\frac{\pi}{4}$ or $T$ is an isosceles triangle with the vertex angle $\frac{\pi}{6} < \theta < \frac{\pi}{2}$.*

If all the elements of initial mesh $\mathcal{T}_0$ satisfy Condition A, we say $\mathcal{T}_0$ satisfies Condition A.

[①]Since two level meshes are not nested. Some quantities like $\nabla v|_T$ or $\nabla v|_E$ in the proof of lemma 4.1, lemma 4.2 and lemma 5.1 may be piecewise constant on some triangle $T$ or edge $E$. Hence we define the edge jump in a larger space $W_{\mathcal{T}_k}$ not merely on $V_k$. However there is no confusion since the edge jump is well-defined.

## 3. Red-green Refinement

This section describes the red-green refinement. In the adaptive loop, the fourth step is to refine the current mesh based on some marked elements. This procedure involves splitting a triangle into smaller ones which may cause hangings nodes. To removing the possible hanging nodes, one way is to use the so called the red-green refinement. This refinement method is used in the code "ConchaBase"(R. Beck) and "PLTMG"(R. E. Bank)[②]

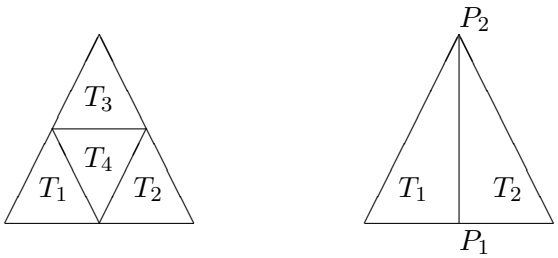


Figure 1. (left)Red-refinement of element domain $T = T_1 \cup T_2 \cup T_3 \cup T_4$ into 4 congruent subdomains $T_1, \ldots, T_4$; (right)Green-refinement of element domain $T = T_1 \cup T_2$ into two children $T_1$ and $T_2$ by connecting the vertex and the midpoint of its corresponding opposite edge.

To give a brief description of the refinement method, we paint all elements in the initial mesh $\mathcal{T}_0$ by the red color.

**Algorithm 1** (Red-Green Refinement)**.** *Input: Triangulation $\mathcal{T}_k$ with the set of marked elements $\mathcal{M}_k$.*

(1) *Divide the set $\mathcal{M}_k$ into two subsets $\mathcal{M}_k^{red} := \{T \in \mathcal{M}_k,$ its color is red$\}$ and $\mathcal{M}_k^{green} := \{T \in \mathcal{M}_k,$ its color is green$\}$;*
(2) *Refine all elements in the red set $\mathcal{M}_k^{red}$ by the red-refinement strategy illustrated on the left hand side of Figure 1 and paint their four children by the red color;*
(3) *Coarsen the elements in the green set $\mathcal{M}_k^{green}$ by removing their fathers' mid-lines, for instance $\overline{P_1P_2}$, on the right hand side of Figure 1, and refine their fathers by the red-refinement and repaint their sons by the red color;*
(4) *Remove the possible hanging nodes by the following strategies until no hanging nodes in the current mesh:*
   (a) *Refine the red elements with at least two hanging nodes by the red-refinement and paint their sons by the red color;*
   (b) *Coarsen the green elements with at least one hanging node by removing their fathers' mid-lines, and refine their fathers by the red-refinement and repaint their sons by the red color;*
   (c) *Refine the red elements with only one hanging node by the green-refinement illustrated on the right hand side of Figure 1 and repaint their children by the green color.*

*Output: The refined conforming triangulation $\mathcal{T}_{k+1} = REFINE(\mathcal{T}_k, \mathcal{M}_k)$.*

A pleasant feature of the resulted meshes with this red-green refinement is that all red triangles are geometrically similar to their ancestors in the initial mesh $\mathcal{T}_0$ and thereby the element quality of these triangles is the same as the quality of their ancestors. Moreover,

[②]The "PLTMG" package after the version 8.0 has changed data structures to use the longest-edge bisection while the previous versions is based on the red-green refinement.

with a hierarchical memory representation, the refining and coarsening can be handled easily. We refer the interested readers to [11, 15, 18, 20, 25] for further details of the red-green refinement.

Let $\mathcal{T}_{k+1}$ be a mesh refined from $\mathcal{T}_k$ by a local refinement, we denote by $\mathcal{R}_k := \mathcal{T}_k \backslash \mathcal{T}_{k+1}$ the set of elements which are refined in the refinement from $\mathcal{T}_k$ to $\mathcal{T}_{k+1}$. Note that $\mathcal{M}_k \subset \mathcal{R}_k$.

## 4. Estimator reduction

This section shows one of main ingredients, namely the reduction of the estimator.

**Lemma 4.1.** *Let $V_k$ and $V_{k+1}$ be the discrete spaces over the triangulations $\mathcal{T}_k$ and $\mathcal{T}_{k+1}$ respectively. There exists a constant $C_3 > 0$ depending on the minimum angle of $\mathcal{T}_0$ and the data $\boldsymbol{A}$ such that*

$$\eta_{k+1}(v,T) \le \eta_{k+1}(w,T) + C_3|v-w|_{1,\omega_T} \text{ for all } T \in \mathcal{T}_{k+1}, w \in V_k, v \in V_{k+1}. \tag{4.1}$$

**Proof :** Since $\nabla w$ is constant on $E$ for any $E \in \mathcal{E}_{k+1}$ (possibly piecewise, see $\overline{A_4A_5}$ of Figure 3 for example in Section 5), $J(w)|_E$ is well-defined. We use the triangle inequality to get

$$\begin{aligned}
\eta_{k+1}(v,T) &= (h_T^2\|f\|_{0,T}^2 + h_T\|J(v)\|_{0,\partial T\cap\Omega}^2)^{\frac{1}{2}} \\
&\le (h_T^2\|f\|_{0,T}^2 + h_T(\|J(w)\|_{0,\partial T\cap\Omega} + \|J(v-w)\|_{0,\partial T\cap\Omega})^2)^{\frac{1}{2}} \\
&\le (h_T^2\|f\|_{0,T}^2 + h_T\|J(w)\|_{0,\partial T\cap\Omega}^2)^{\frac{1}{2}} + h_T^{1/2}\|J(v-w)\|_{0,\partial T\cap\Omega} \\
&= \eta_{k+1}(w,T) + h_T^{1/2}\|J(v-w)\|_{0,\partial T\cap\Omega}.
\end{aligned} \tag{4.2}$$

Let $E = \overline{T} \cap \overline{T'}$ and $\overrightarrow{n_E}$ and $\overrightarrow{n_E}'$ be the unit outer normals of $\partial T$ and $\partial T'$ restricted on $E$. Note that the quantities $\mathbf{A}\nabla(v-w)|_T$ and $\mathbf{A}\nabla(v-w)|_{T'}$ may also be piecewise constant on $T$ and $T'$; c.f. the edge $\overline{A_4A_5}$ of Figure 3 in Section 5. Then using the scaling argument, the (possibly piecewise) trace and inverse inequalities, one can get

$$\|\mathbf{A}\nabla(v-w)|_T\|_{0,E} \le Ch_T^{-1/2}\|\nabla(v-w)\|_{0,T}. \tag{4.3}$$

and

$$\|\mathbf{A}\nabla(v-w)|_{T'}\|_{0,E} \le Ch_{T'}^{-1/2}\|\nabla(v-w)\|_{0,T'}. \tag{4.4}$$

Hence

$$\begin{aligned}
\|J(v-w)\|_{0,E} &= \|\mathbf{A}\nabla(v-w)|_T \cdot \overrightarrow{n_E} + \mathbf{A}\nabla(v-w)|_{T'} \cdot \overrightarrow{n_E}'\|_{0,E} \\
&\le Ch_T^{-1/2}|v-w|_{1,\omega_E}.
\end{aligned} \tag{4.5}$$

Inserting (4.5) into (4.2) ends the proof. □

**Lemma 4.2** (estimator reduction)**.** *Let $\mathcal{T}_{k+1}$ be some refinement of $\mathcal{T}_k$ in the sense of Algorithm 1. There exist constants $0 < \lambda < 1$ and $C_4 > 0$ depending on the minimum angle of $\mathcal{T}_0$ and the data $\boldsymbol{A}$ with*

$$\eta_{k+1}^2(v_{k+1},\mathcal{T}_{k+1}) \le (1+\delta)\eta_k^2(v_k,\mathcal{T}_k) - \lambda(1+\delta)\eta_k^2(v_k,\mathcal{M}_k) + C_4(1+1/\delta)\,|||\, v_{k+1}-v_k|||^2\ ,$$

*for any $v_k \in V_k$ and $v_{k+1} \in V_{k+1}$ with the parameter $\delta > 0$ to be determined below.*

*Proof.* Applying Lemma 4.1 with $v_k \in V_k$, $v_{k+1} \in V_{k+1}$ over $T \in \mathcal{T}_{k+1}$, and using Young's inequality with the parameter $\delta$, we derive

$$\eta_{k+1}^2(v_{k+1},T) \le (1+\delta)\eta_{k+1}^2(v_k,T) + C_3(1+1/\delta)|v_{k+1}-v_k|_{1,\omega_T}^2\ .$$

Due to the finite overlapping of $\omega_T$ and the equivalence of the $H^1$ norm and the energy norm in $\Omega$, the summation over all elements $T \in \mathcal{T}_{k+1}$ leads to

$$\eta^2_{k+1}(v_{k+1}, \mathcal{T}_{k+1}) \quad \leq \quad (1+\delta)\eta^2_{k+1}(v_k, \mathcal{T}_{k+1}) + C(1+1/\delta)|||v_{k+1} - v_k|||^2 \ .$$

In what follows we plan to bound the first term on the right hand side of the above inequality by the estimator on the mesh $\mathcal{T}_k$. To this end, we need to take care of three cases.

Case 1. $T \in \mathcal{M}_k \subset \mathcal{T}_k$ and $T$ is a green element. From Algorithm 1, we know green elements appear in pairs. Hence there exits another green element $T'$ which adjoins to $T$ with $E = T \cap T'$. We define $\tilde{\mathcal{M}}_k^{\text{green}} := \{T' |\ T \in \mathcal{M}_k^{\text{green}}\}$ and $\tilde{\mathcal{M}}_k := \mathcal{M}_k \cup \tilde{\mathcal{M}}_k^{\text{green}}$. Let $K = T \cup T'$ and $\mathcal{T}_{k+1,K} := \{\tilde{T} \in \mathcal{T}_{k+1} \mid \tilde{T} \subset K\}$ (see Figure 2). It follows the definition of the element-size that

$$h_{\tilde{T}} = |\tilde{T}|^{1/2} \leq (1/4|K|)^{1/2} \quad \text{and} \quad h_T = h_{T'} = |T|^{1/2} = (1/2|K|)^{1/2} \ .$$

This yields

$$h_{\tilde{T}} \leq 2^{-1/2} h_T = 2^{-1/2} h_{T'}. \tag{4.6}$$

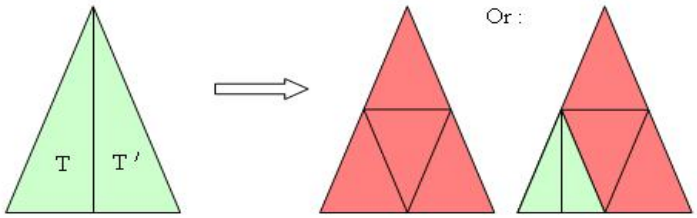


FIGURE 2. $K = T \cup T'$ and $\mathcal{T}_{k+1,K}$.

Define $\mathcal{E}_{k+1,K} := \{e \in \mathcal{E}_{k+1} |\ e \subset \partial\tilde{T} \backslash \partial K, \forall \tilde{T} \in \mathcal{T}_{k+1,K}\}$. Given $e \in \mathcal{E}_{k+1,K}$, although $\nabla v_k$ may be piecewise constant on $e$, one has $J(v_k)|_e = 0$. This and (4.6) lead to

$$\begin{aligned}\eta^2_{k+1}(v_k, K) = \sum_{\tilde{T} \in \mathcal{T}_{k+1,K}} \eta^2_{k+1}(v_k, \tilde{T}) &\leq 2^{-1} h_T^2 \|f\|^2_{0,K} + 2^{-1/2} \sum_{e \in \mathcal{E}_{k+1} \cap \partial K} h_T \|J(v_k)|_e\|^2_{0,e} \\ &\leq 2^{-1/2}\eta^2_k(v_k, T) + 2^{-1/2}\eta^2_k(v_k, T') = 2^{-1/2}\eta^2_k(v_k, K).\end{aligned}$$

Case 2. $T \in \mathcal{M}_k \subset \mathcal{T}_k$ and $T$ is a red element. For this case, a similar argument of the Case 1 shows

$$\eta^2_{k+1}(v_k, T) \leq 2^{-1/2}\eta^2_k(v_k, T).$$

Case 3. $T \in \mathcal{T}_{k+1} \backslash \tilde{\mathcal{M}}_k$ with $\tilde{\mathcal{M}}_k$ defined in Case 1. If $T$ is not refined, we have $\eta_{k+1}(v_k, T) = \eta_k(v_k, T)$; if $T$ is refined we can use the same arguments of Cases 1 and 2 to prove $\eta_{k+1}(v_k, T) \leq \eta_k(v_k, T)$. Therefore, for both cases, we have

$$\eta_{k+1}(v_k, T) \leq \eta_k(v_k, T).$$

Taking aforementioned three cases into account and summing over all $T \in \mathcal{T}_{k+1}$ leads to

$$\begin{aligned}\eta^2_{k+1}(v_k, \mathcal{T}_{k+1}) &= \eta^2_{k+1}(v_k, \mathcal{T}_{k+1} \backslash \tilde{\mathcal{M}}_k) + \eta^2_{k+1}(v_k, \tilde{\mathcal{M}}_k) \\ &\leq \eta^2_k(v_k, \mathcal{T}_k \backslash \tilde{\mathcal{M}}_k) + 2^{-1/2}\eta^2_k(v_k, \tilde{\mathcal{M}}_k) \\ &\leq \eta^2_k(v_k, \mathcal{T}_k) - (1 - 2^{-1/2})\eta^2_k(v_k, \tilde{\mathcal{M}}_k) \\ &\leq \eta^2_k(v_k, \mathcal{T}_k) - (1 - 2^{-1/2})\eta^2_k(v_k, \mathcal{M}_k) \ .\end{aligned}$$

The choice $\lambda = 1 - 2^{-1/2} \in (0,1)$ ends the proof. □

## 5. Quasi-orthogonality

This section presents the quasi-orthogonality. Let $\Omega|_{\mathcal{R}_k} = \bigcup_{T\in\mathcal{R}_k} T$ and $\mathcal{P}_{k+1} := \{T \in \mathcal{T}_{k+1} |\ T \subset \Omega|_{\mathcal{R}_k}\}$.

**Lemma 5.1.** *(quasi-orthogonality) Assume $\mathcal{T}_0$ satisfies Condition A. Let $\mathcal{T}_{k+1}$ be some refinement of $\mathcal{T}_k$ with Algorithm 1. There exist constants $0 < \rho_0 < 1$ and $C_5 > 0$ depending on the minimum angle of $\mathcal{T}_0$ and the data $\boldsymbol{A}$ such that*

$$|a(u-u_{k+1}, u_{k+1}-u_k)| \le (\gamma + \frac{\rho_0}{2}) \,|||\, u_{k+1}-u_k \,|||^2 + \frac{C_5}{\gamma} \sum_{T\in\mathcal{R}_k} h_T^2 \|f\|_{0,T}^2 \ . \tag{5.1}$$

*where the parameter $\gamma > 0$ is to be determined later.*

*Proof.* Let $I_{k+1}$ be the Lagrange interpolator associated to $\mathcal{T}_{k+1}$, then one can use Green' formula to get

$$\begin{aligned} a(u-u_{k+1}, u_{k+1}-u_k) &= a\big(u-u_{k+1}, (I-I_{k+1})(u_{k+1}-u_k)\big) \\ &= \big(f, (I-I_{k+1})(u_{k+1}-u_k)\big) - a\big(u_{k+1}, (I-I_{k+1})(u_{k+1}-u_k)\big) \\ &= \sum_{T\in\mathcal{P}_{k+1}} \big(f, (I-I_{k+1})(u_{k+1}-u_k)\big)_T \\ &\quad - \sum_{T\in\mathcal{P}_{k+1}} \sum_{e\subset\partial T} \int_e [\![\mathbf{A}\nabla u_{k+1}]\!]\cdot\overrightarrow{n_e}((I-I_{k+1})(u_{k+1}-u_k))ds. \end{aligned} \tag{5.2}$$

Since $(I-I_{k+1})(u_{k+1}-u_k)(p) = 0$ for any node $p$ of $\mathcal{T}_{k+1}$, one can use the elementwise Cauchy-Schwarz inequality with respect to $\mathcal{T}_{k+1}$ and the scaling argument to obtain

$$\begin{aligned} \sum_{T\in\mathcal{P}_{k+1}} \big(f, (I-I_{k+1})(u_{k+1}-u_k)\big)_T &\le \sum_{T\in\mathcal{P}_{k+1}} \|f\|_{0,T} \|(I-I_{k+1})(u_{k+1}-u_k)\|_{0,T} \\ &\le C_8 \sum_{T\in\mathcal{P}_{k+1}} h_T \|f\|_{0,T} |u_{k+1}-u_k|_{1,T}. \end{aligned}$$

For a pair of green elements $T$ and $T'$, we set $K = T \cup T'$ (see Figure 3). We denote by $G_k$ the set of the central lines of their fathers, for instance, the line $\overline{A_4A_5}$ depicted in the Figure 3. Hence we can derive as

$$\begin{aligned} a(u-u_{k+1}, u_{k+1}-u_k) &\le C_8 \sum_{T\in\mathcal{P}_{k+1}} h_T \|f\|_{0,T} |u_{k+1}-u_k|_{1,T} \\ &\quad - \sum_{E\in G_k} ([\![\mathbf{A}\nabla u_{k+1}]\!]\cdot\overrightarrow{n_E}) \int_E (I-I_{k+1})(u_{k+1}-u_k)ds. \end{aligned} \tag{5.3}$$

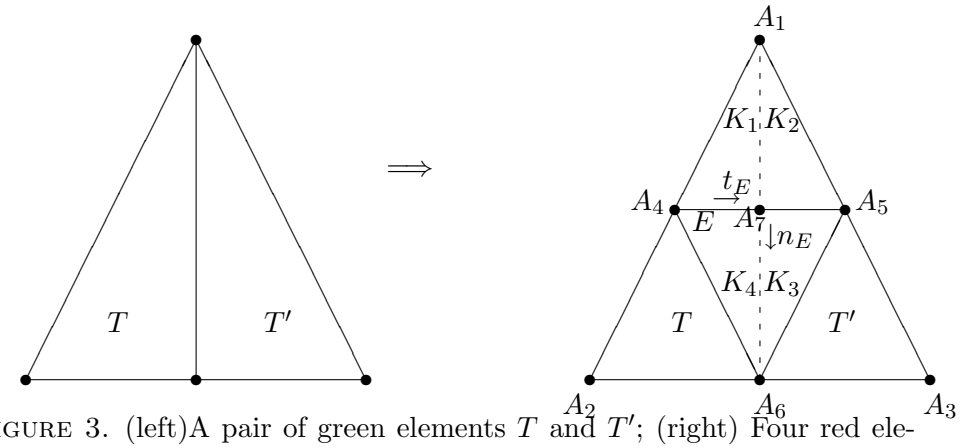


FIGURE 3. (left)A pair of green elements $T$ and $T'$; (right) Four red elements refined from their father.

Using Young's inequality with parameter $\varepsilon > 0$ and the equivalence of the $H^1$ norm and energy norm in $\Omega$, we can obtain

$$\begin{aligned}\sum_{T\in\mathcal{P}_{k+1}} h_T\|f\|_{0,T}|u_{k+1}-u_k|_{1,T} &\le \varepsilon|u_{k+1}-u_k|^2_{1,\Omega|\mathcal{R}_k} + \frac{1}{4\varepsilon}\sum_{T\in\mathcal{P}_{k+1}} h_T^2\|f\|^2_{0,T}\\ &\le \varepsilon|u_{k+1}-u_k|^2_{1,\Omega} + \frac{1}{4\varepsilon}\sum_{T\in\mathcal{R}_k} h_T^2\|f\|^2_{0,T}\\ &\le C_a^2\varepsilon\,|||\,u_{k+1}-u_k\,|||^2 + \frac{1}{4\varepsilon}\sum_{T\in\mathcal{R}_k} h_T^2\|f\|^2_{0,T}.\end{aligned}$$

It remains to bound the second term on the right-hand side of (5.3). If $E \in \mathcal{E}_{k+1}\backslash\mathcal{E}_k$ lies in the interior of some $T \in \mathcal{T}_k$ (see $\overline{A_4A_6}$ in Figure 3) one has $(I - I_{k+1})u_k|_E = 0$; if $E \in \mathcal{E}_{k+1}\backslash\mathcal{E}_k$ is a child of some edge in $\mathcal{E}_k$ (see $\overline{A_1A_4}$ in Figure 3), $(I - I_{k+1})u_k|_E = 0$; if $E \in \mathcal{E}_{k+1} \cap \mathcal{E}_k$, $(I - I_{k+1})u_k|_E = 0$. Therefore, we only need to consider edge $E \in \mathcal{E}_{k+1}\backslash\mathcal{E}_k$ which is not contained in any $T \in \mathcal{T}_k$, for instance, $E = \overline{A_4A_5}$ in Figure 3. Because of $(I - I_{k+1})u_{k+1} \equiv 0$, we get

$$\int_E (I - I_{k+1})(u_{k+1} - u_k)ds = -\int_E (I - I_{k+1})u_k ds.$$

Since $((I - I_{k+1})u_k)(A_4) = 0$, $((I - I_{k+1})u_k)(A_5) = 0$ and $(I - I_{k+1})u_k$ is a piecewise linear function on $E$, one can use the trapezoidal quadrature rule on $\overline{A_4A_7}$ and $\overline{A_7A_5}$, respectively, to get

$$\begin{aligned}&\int_E (I - I_{k+1})(u_{k+1} - u_k)ds\\ =\ & -\left(\frac{0 + ((I - I_{k+1})u_k)(A_7)}{2}\frac{h_E}{2} + \frac{((I - I_{k+1})u_k)(A_7) + 0}{2}\frac{h_E}{2}\right)\\ =\ & -\frac{h_E}{2}\big(u_k(A_7) - (I_{k+1}u_k)(A_7)\big),\end{aligned}$$

with the length $h_E$ of $E$. Since $u_k$ is linear on $\overline{A_1A_6}$ and $A_7$ is the midpoint of $\overline{A_1A_6}$, we have

$$\int_E (I-I_{k+1})(u_{k+1}-u_k)ds = -\frac{h_E}{4}\Big(u_k(A_1)+u_k(A_6)-u_k(A_4)-u_k(A_5)\Big). \tag{5.4}$$

The continuity of $\nabla u_{k+1}\cdot\overrightarrow{t_E}$ over $E$, i.e., $\nabla u_{k+1}|_{K_1\cup K_2}\cdot\overrightarrow{t_E}=\nabla u_{k+1}|_{K_3\cup K_4}\cdot\overrightarrow{t_E}$, yields

$$\begin{aligned}
&\big(u_k(A_1)+u_k(A_6)-u_k(A_4)-u_k(A_5)\big)\\
&=\frac{1}{2}\big(u_k(A_1)-u_k(A_4)+u_k(A_6)-u_k(A_4)+u_k(A_1)-u_k(A_5)+u_k(A_6)-u_k(A_5)\big)\\
&=\frac{1}{2}\big(\nabla u_k|_T\cdot\overrightarrow{A_4A_1}+\nabla u_k|_T\cdot\overrightarrow{A_4A_6}+\nabla u_k|_{T'}\cdot\overrightarrow{A_5A_1}+\nabla u_k|_{T'}\cdot\overrightarrow{A_5A_6}\big)\\
&=\frac{1}{2}\big(\nabla u_k|_T\cdot\overrightarrow{A_4A_5}+\nabla u_k|_{T'}\cdot\overrightarrow{A_5A_4}\big)=\frac{h_E}{2}\big(\nabla u_k|_T\cdot\overrightarrow{t_E}-\nabla u_k|_{T'}\cdot\overrightarrow{t_E}\big)\\
&=-\frac{h_E}{2}\big(\nabla(u_{k+1}-u_k)|_{K_1\cup K_4}\cdot\overrightarrow{t_E}-\nabla(u_{k+1}-u_k)|_{K_2\cup K_3}\cdot\overrightarrow{t_E}\big).
\end{aligned}$$

Using the fact that $\nabla u_{k+1}|_{K_1}\cdot\overrightarrow{t_E}=\nabla u_{k+1}|_{K_4}\cdot\overrightarrow{t_E}$ and that $\nabla u_{k+1}|_{K_2}\cdot\overrightarrow{t_E}=\nabla u_{k+1}|_{K_3}\cdot\overrightarrow{t_E}$, and inserting the above identity into (5.4) leads to

$$\begin{aligned}
&(\llbracket\mathbf{A}\nabla u_{k+1}\rrbracket\cdot\overrightarrow{n_E})\int_E(I-I_{k+1})(u_{k+1}-u_k)ds\\
&=\frac{h_E^2}{8}\big(\mathbf{A}\nabla u_{k+1}|_{K_1\cup K_2}\cdot\overrightarrow{n_E}-\mathbf{A}\nabla u_{k+1}|_{K_3\cup K_4}\cdot\overrightarrow{n_E}\big)\\
&\quad\times\big(\nabla(u_{k+1}-u_k)|_{K_1\cup K_4}\cdot\overrightarrow{t_E}-\nabla(u_{k+1}-u_k)|_{K_2\cup K_3}\cdot\overrightarrow{t_E}\big)\\
&=\frac{h_E^2}{8}\Big(\big(\mathbf{A}\nabla u_{k+1}|_{K_1}\cdot\overrightarrow{n_E}\big)\big(\nabla(u_{k+1}-u_k)|_{K_1}\cdot\overrightarrow{t_E}\big)\\
&\quad-\big(\mathbf{A}\nabla u_{k+1}|_{K_2}\cdot\overrightarrow{n_E}\big)\big(\nabla(u_{k+1}-u_k)|_{K_2}\cdot\overrightarrow{t_E}\big)\\
&\quad+\big(\mathbf{A}\nabla u_{k+1}|_{K_3}\cdot\overrightarrow{n_E}\big)\big(\nabla(u_{k+1}-u_k)|_{K_3}\cdot\overrightarrow{t_E}\big)\\
&\quad-\big(\mathbf{A}\nabla u_{k+1}|_{K_4}\cdot\overrightarrow{n_E}\big)\big(\nabla(u_{k+1}-u_k)|_{K_4}\cdot\overrightarrow{t_E}\big)\Big).
\end{aligned}\tag{5.5}$$

Using $\nabla u_{k+1}|_{K_1}\cdot\overrightarrow{t_E}=\nabla u_{k+1}|_{K_4}\cdot\overrightarrow{t_E}$ and $\nabla u_{k+1}|_{K_2}\cdot\overrightarrow{t_E}=\nabla u_{k+1}|_{K_3}\cdot\overrightarrow{t_E}$ again gives

$$\begin{aligned}
&\big(\mathbf{A}\nabla u_k|_{K_1}\cdot\overrightarrow{n_E}\big)\big(\nabla(u_{k+1}-u_k)|_{K_1}\cdot\overrightarrow{t_E}\big)-\big(\mathbf{A}\nabla u_k|_{K_2}\cdot\overrightarrow{n_E}\big)\big(\nabla(u_{k+1}-u_k)|_{K_2}\cdot\overrightarrow{t_E}\big)\\
&\quad+\big(\mathbf{A}\nabla u_k|_{K_3}\cdot\overrightarrow{n_E}\big)\big(\nabla(u_{k+1}-u_k)|_{K_3}\cdot\overrightarrow{t_E}\big)-\big(\mathbf{A}\nabla u_k|_{K_4}\cdot\overrightarrow{n_E}\big)\big(\nabla(u_{k+1}-u_k)|_{K_4}\cdot\overrightarrow{t_E}\big)=0.
\end{aligned}\tag{5.6}$$

Combining (5.5) and (5.6) leads to

$$\begin{aligned}
&(\llbracket\mathbf{A}\nabla u_{k+1}\rrbracket\cdot\overrightarrow{n_E})\int_E(I-I_{k+1})(u_{k+1}-u_k)\mathsf{ds}\\
=\;&\frac{h_E^2}{8}\Big(\big(\mathbf{A}\nabla(u_{k+1}-u_k)|_{K_1}\cdot\overrightarrow{n_E}\big)\big(\nabla(u_{k+1}-u_k)|_{K_1}\cdot\overrightarrow{t_E}\big)\\
&-\big(\mathbf{A}\nabla(u_{k+1}-u_k)|_{K_2}\cdot\overrightarrow{n_E}\big)\big(\nabla(u_{k+1}-u_k)|_{K_2}\cdot\overrightarrow{t_E}\big)\\
&+\big(\mathbf{A}\nabla(u_{k+1}-u_k)|_{K_3}\cdot\overrightarrow{n_E}\big)\big(\nabla(u_{k+1}-u_k)|_{K_3}\cdot\overrightarrow{t_E}\big)\\
&-\big(\mathbf{A}\nabla(u_{k+1}-u_k)|_{K_4}\cdot\overrightarrow{n_E}\big)\big(\nabla(u_{k+1}-u_k)|_{K_4}\cdot\overrightarrow{t_E}\big)\Big).
\end{aligned}$$

Let $\theta_1$ denote the angle between the gradient $\nabla(u_{k+1}-u_k)|_{K_1}$ and the normal vector $\overrightarrow{n_E}$ which implies that the angle between the gradient $\nabla(u_{k+1}-u_k)|_{K_1}$ and the tangent vector $\overrightarrow{t_E}$ is either $\pi/2-\theta_1$ or $\pi/2+\theta_1$. Whence we derive

$$\begin{aligned}
& (\mathbf{A}\nabla(u_{k+1}-u_k)|_{K_1}\cdot\overrightarrow{n_E})(\nabla(u_{k+1}-u_k)|_{K_1}\cdot\overrightarrow{t_E}) \\
= \ & \big(\mathbf{A}\big|\nabla(u_{k+1}-u_k)|_{K_1}\big|\cos\theta_1\big)\big(\pm\big|\nabla(u_{k+1}-u_k)|_{K_1}\big|\sin\theta_1\big) \\
= \ & \pm\frac{1}{2}\big|\mathbf{A}^{\frac{1}{2}}\nabla(u_{k+1}-u_k)\big|^2\sin 2\theta_1 \\
= \ & \pm\frac{\sin 2\theta_1}{2|K_1|}\,|||\,u_{k+1}-u_k\,|||^2_{K_1}\,.
\end{aligned}$$

This implies

$$|(\mathbf{A}\nabla(u_{k+1}-u_k)|_{K_1}\cdot\overrightarrow{n_E})(\nabla(u_{k+1}-u_k)|_{K_1}\cdot\overrightarrow{t_E})|\le\frac{4}{|K|}\,|||\,u_{k+1}-u_k\,|||^2_{K_1}\,.$$

A similar argument leads to

$$|(\mathbf{A}\nabla(u_{k+1}-u_k)|_{K_i}\cdot\overrightarrow{n_E})(\nabla(u_{k+1}-u_k)|_{K_i}\cdot\overrightarrow{t_E})|\le\frac{4}{|K|}\,|||\,u_{k+1}-u_k|||^2_{K_i}, i=2,3,4.$$

Let $S=K_1\cup K_2\cup K_3\cup K_4$ and $l=|\overline{A_2A_3}|$ and $h_l$ be the height on edge $\overline{A_2A_3}$ in $K$, then $S\subset K$ and $h_E=l/2$. Setting $\rho_0=\sup_{T\in\mathcal{T}_0}\rho(T)$. The condition on $\mathcal{T}_0$ implies $0<\rho_0<1$. Therefore

$$\begin{aligned}
& |\int_E([\![\mathbf{A}\nabla u_{k+1}]\!]\cdot\overrightarrow{n_E})(I-I_{k+1})(u_{k+1}-u_k)ds| \\
& \quad\le\frac{l^2}{8|K|}\,|||\,u_{k+1}-u_k|||^2_S=\frac{l}{4h_l}\,|||\,u_{k+1}-u_k|||^2_S\le\frac{1}{2}\rho_0\,|||\,u_{k+1}-u_k\,|||^2_S\,.
\end{aligned}$$

Taking $\gamma=C_8C_a^2\varepsilon$ and $C_5=\frac{C_8^2C_a^2}{4}$, the summation over $E\in G_k$ ends the proof. □

## 6. Convergence

This section proves the convergence of the adaptive conforming $P_1$ method with the red-green refinement strategy.

AFEM Algorithm: Given the initial grid $\mathcal{T}_0$ and parameters $0<\theta,\ \tilde{\theta}<1$ and $\varepsilon$.
$[\mathcal{T}_N,u_N]=$ AFEM($\mathcal{T}_0,\ f,\ \varepsilon,\ \theta,\ \tilde{\theta}$). set $k:=0$, $\eta=\varepsilon$.
While $\eta\ge\varepsilon$,

(1) Solve (2.4) on $\mathcal{T}_k$ to get the solution $u_k$;
(2) Compute the error estimator $\eta=\eta_{\mathcal{T}_k}(u_k,\mathcal{T}_k)$;
(3) Mark the minimal element set $\mathcal{M}_k$ such that

$$\eta_k(u_k,\mathcal{M}_k)\ge\theta\eta_k(u_k,\mathcal{T}_k); \tag{6.1}$$

(4) If it is necessary, enlarge $\mathcal{M}_k$ (still denoted by $\mathcal{M}_k$) such that

$$\sum_{T\in\mathcal{M}_k}h_T^2\|f\|^2_{0,T}\ge\tilde{\theta}\sum_{T\in\mathcal{T}_k}h_T^2\|f\|^2_{0,T}; \tag{6.2}$$

(5) Refine the elements in $\mathcal{M}_k$ by Algorithm 1 to get $\mathcal{T}_{k+1}$;
(6) Set $k=k+1$.

End While

$\mathcal{T}_N = \mathcal{T}_k$, $u_N = u_k$.

End AFEM

Set $e_{k+1} = |||u - u_{k+1}|||$, $e_k = |||u - u_k|||$ and $e_{k,k+1} = |||u_k - u_{k+1}|||$. The following theorem highlights on the relation of errors between two level meshes.

**Lemma 6.1** (Error contraction)**.** *Assume $\mathcal{T}_0$ satisfies Condition A. Let $\mathcal{T}_{k+1} = REFINE(\mathcal{T}_k, \mathcal{M}_k)$ with* (6.1)*. Then there exist constants $0 < \alpha < 1$, $\beta > 0$, and $C_6 > 0$ such that*

$$e_{k+1}^2 + \beta\eta_{k+1}^2 \le \alpha(e_k^2 + \beta\eta_k^2) + C_6 \sum_{T\in\mathcal{R}_k} h_T^2 \|f\|_{0,T}^2 \ . \tag{6.3}$$

*Proof.* It follows from the quasi-orthogonality of Lemma 5.1 and the estimator reduction of Lemma 4.2 that

$$\begin{aligned} e_{k+1}^2 + \beta\eta_{k+1}^2 &= e_k^2 - e_{k,k+1}^2 - 2a(u - u_{k+1}, u_{k+1} - u_k) + \beta\eta_{k+1}^2 \\ &\le e_k^2 - e_{k,k+1}^2 + 2\gamma e_{k,k+1}^2 + \frac{2C_5}{\gamma} \sum_{T\in\mathcal{R}_k} h_T^2 \|f\|_{0,T}^2 + \rho_0 e_{k,k+1}^2 \\ &\quad +\beta\bigg((1+\delta)\eta_k^2 - \lambda(1+\delta)\eta_k^2(u_k, \mathcal{M}_k) + C_4(1+1/\delta)e_{k,k+1}^2\bigg). \end{aligned}$$

The bulk criterion (6.1) and the reliability of the estimator give

$$\begin{aligned} -\beta\lambda(1+\delta)\eta_k^2(u_k, \mathcal{M}_k) &\le -\theta\beta\lambda(1+\delta)\eta_k^2 \\ &= -\theta\beta\lambda(1+\delta)(1-s+s)\eta_k^2 \\ &\le -\frac{\theta\beta\lambda(1+\delta)s}{C_1} e_k^2 - \theta\beta\lambda(1+\delta)(1-s)\eta_k^2, \end{aligned}$$

with the constant $0 < s < 1$ to be determined later. Inserting this estimate into the previous one leads to

$$\begin{aligned} e_{k+1}^2 + \beta\eta_{k+1}^2 &\le \bigg(1 - \frac{\theta\beta\lambda(1+\delta)s}{C_1}\bigg)e_k^2 + \beta\bigg((1+\delta)(1-\theta\lambda(1-s))\bigg)\eta_k^2 \\ &\quad -\bigg(1 - \rho_0 - 2\gamma - \beta C_4(1+1/\delta)\bigg)e_{k,k+1}^2 + \frac{2C_5}{\gamma} \sum_{T\in\mathcal{R}_k} h_T^2 \|f\|_{0,T}^2. \end{aligned}$$

It remains to choose these parameters. First we select $0 < \delta < 1$ such that $\alpha = \max((1+\delta)(1-\lambda\theta(1-s)), 1 - \frac{\theta\beta\lambda(1+\delta)s}{C_1}) < 1$. Then the choice $\beta = (1 - \rho_0 - 2\gamma)/C_4(1+1/\delta)$ with $2\gamma < 1 - \rho_0$ ends the proof. □

**Lemma 6.2.** *Let $\mathcal{T}_{k+1}$ be some refinement of $\mathcal{T}_k$ with* (6.2)*. There exists $0 < \mu < 1$ with*

$$\sum_{T\in\mathcal{T}_{k+1}} h_T^2 \|f\|_{0,T}^2 \le \mu \sum_{T\in\mathcal{T}_k} h_T^2 \|f\|_{0,T}^2. \tag{6.4}$$

*Proof.* The result follows from the bulk criterion (6.2) and the definition of the element-size. □

**Theorem 6.3** (Convergence)**.** *Assume $\mathcal{T}_0$ satisfies Condition A. Let $(\mathcal{T}_k, u_k)$ be the sequence of meshes and solutions produced by the AFEM Algorithm. Then there exist constants $0 < \xi < 1$, $\beta > 0$, and $C_7 > 0$ such that*

$$e_k^2 + \beta\eta_k^2 \le C_7 \xi^k. \tag{6.5}$$

*Proof.* Set $E_k = e_k^2 + \beta\eta_k^2$ and $H_k(f) = \sum_{T\in\mathcal{T}_k} h_T^2\|f\|_{0,T}^2$, $k = 1, 2, \cdots, N$.

Combining Lemma 6.1 and Lemma 6.2 yields

$$\begin{aligned} E_k &\leq \alpha E_{k-1} + C_6 H_{k-1}(f) \\ &\leq \alpha(\alpha E_{k-2} + C_6 H_{k-2}(f)) + C_6\mu H_{k-2}(f) \\ &\leq \alpha^k E_0 + C_6 H_0(f)\sum_{i=0}^{k-1}\alpha^i\mu^{k-1-i}. \end{aligned}$$

Taking $\max(\alpha,\mu) < \xi < 1$, we have

$$\sum_{i=0}^{k-1}\alpha^i\mu^{k-1-i} \leq \frac{\xi^k}{\xi - \min(\alpha,\mu)}.$$

Setting $C_7 = |u-u_0|_{1,\Omega}^2 + \beta\eta_0^2 + \frac{C_6\sum_{T\in\mathcal{T}_0} h_T^2\|f\|_{0,T}^2}{\xi-\min(\alpha,\mu)}$ completes the proof. □

## 7. Modified red-green refinement

This section presents a modified red-green refinement. With such a refinement strategy, one can prove the convergence of the adaptive algorithm under a much weaker condition on the initial mesh which reads

Condition B: Given $T$, assume that there exists at least one side (denoted by $a$) such that

$$|h_a| > 1/2|a| \text{ with the height } h_a \text{ on } a. \tag{7.1}$$

**Remark 7.1.** *Let $\alpha$, $\beta$, and $\gamma$ ($\alpha \leq \beta \leq \gamma$) be three angles of $T$. One sufficient condition for Condition B is that either $\gamma < \frac{5\pi}{6}$, or $\gamma \geq \frac{5\pi}{6}$ and $\frac{\sin\beta\sin(\alpha+\beta)}{\sin\alpha} > \frac{1}{2}$. This condition is satisfied by almost all practical meshes. In fact, for one extreme case with $\gamma = 170^o$, $\beta = 8^o$ and $\alpha = 2^o$, one has $\frac{\sin\beta\sin(\alpha+\beta)}{\sin\alpha} \approx 0.6925 > \frac{1}{2}$.*

Now we present the modified red-green refinement. To this end, we let $e_B$ denote the edge of $T$ which satisfies Condition B. We paint all elements in the initial mesh $\mathcal{T}_0$ by the red color.

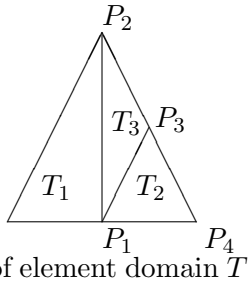


Figure 4. Blue-refinement of element domain $T = T_1 \cup T_2 \cup T_3$ into a child $T_1$ and two grandchildren $T_2$ and $T_3$.

**Algorithm 2** (Modified Red-Green Refinement)**.** *Input: Triangulation $\mathcal{T}_k$ with the set of marked elements $\mathcal{M}_k$.*

1. *Divide $\mathcal{M}_k$ into three subsets $\mathcal{M}_k^{red} := \{T \in \mathcal{M}_k,$ its color is red$\}$, $\mathcal{M}_k^{green} := \{T \in \mathcal{M}_k,$ its color is green$\}$, and $\mathcal{M}_k^{blue} := \{T \in \mathcal{M}_k,$ its color is blue$\}$.*
2. *Refine all elements in $\mathcal{M}_k^{red}$ by the red-refinement strategy and paint its four children by the red color;*

(3) *Coarsen the elements in* $\mathcal{M}_k^{green}$ *by removing their fathers' mid-lines, for instance* $\overline{P_1P_2}$*, on the right hand side of Figure 1, or their fathers' mid-lines and central lines, for instance* $\overline{P_1P_2}$ *and* $\overline{P_1P_3}$ *in Figure 4, and refine their fathers by the red-refinement and repaint their sons by the red color.*
(4) *Coarsen the elements in* $\mathcal{M}_k^{blue}$ *by removing their grandfathers' mid-lines and central lines, for instance* $\overline{P_1P_2}$ *and* $\overline{P_1P_3}$ *in Figure 4, and refine their grandfathers by the red-refinement and repaint their sons by the red color.*
(5) *Remove the possible hanging nodes by the following strategies until no hanging nodes in the current mesh:*
   (a) *Refine the red element with three hanging nodes by the red-refinement and paint their sons by the red color.*
   (b) *Refine the red element* $T$ *with two hanging nodes by the modified blue-refinement: First divide the element into two children by the green-refinement, namely, connecting the midpoint of* $e_B$ *and its opposite vertex, and repaint the children by the green color; Second decompose the child (or two children) generated by the green-refinement with one hanging node into two grandchildren (or four grandchildren) and repaint the grandchildren by the blue color. c.f Figure 4.*
   (c) *Refine the red element* $T$ *with one hanging node with the green-refinement into two children by connecting the midpoint of* $e_B$ *and its opposite vertex and repaint both children by the green color. In the case where the only one hanging node is not on the* $e_B$*, further decompose the child generated by the green-refinement with one hanging node into two grandchildren and repaint both of them by the blue color.*
   (d) *Coarsen the green element with two hanging nodes and refine its father by the red-refinement and repaint the four children by red color.*
   (e) *Refine the green element with one hanging node which is not on the formerly bisected edge by the blue-refinement and repaint its two children by the blue color.*
   (f) *Coarsen the green element with one hanging node which is on the formerly bisected edge and refine its father element by the red-refinement and repaint its four children by the red color.*
   (g) *Coarsen the blue element with one hanging node and refine its grandfather by the red-refinement and repaint the four children by red color.*
(6) *Locally adjust all the local meshes depicted on the left-hand side of Figure 5 to the meshes shown on the right-hand side of Figure 5 by post-processing A.*
(7) *Locally adjust all the local parallelogram meshes illustrated in the middle of Figure 6 to the local parallelogram meshes shown on the right-hand side of Figure 6 with post-processing B.*

*Output: The refined conforming triangulation* $\mathcal{T}_{k+1} = REFINE(\mathcal{T}_k, \mathcal{M}_k)$.

Post-processing A is to improve the regularity of current mesh while post-processing B is useful to prove the quasi-orthogonality in Lemma 5.1.

The convergence of AFEM with the red-green refinement can be extended to the AFEM based on the modified red-green refinement with a slight modification. In fact, the necessary modification is to define the element-size of blue elements as follows:
For blue element $T_2$ or $T_3$ shown in Figure 4, we define the element-size as:

$$h_{T_2} := \sqrt{\kappa|T_2|},\ h_{T_3} := \sqrt{\kappa|T_3|}. \tag{7.2}$$

where constant $\kappa = 3/2$. We will explain the reason in the proof of the following theorem.

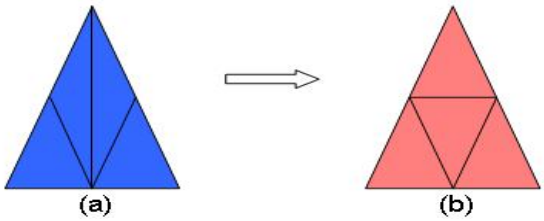


FIGURE 5. Post-processing A: The local mesh on the left-hand side should be locally adjusted to the mesh on the right-hand side.

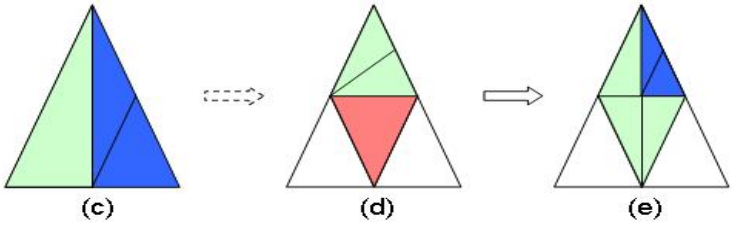


FIGURE 6. Post-processing B: The local parallelogram mesh in the middle of the above figure is generated from the mesh on the left-hand side, but it should be locally adjusted to the mesh shown on the right-hand side of the above figure.

**Theorem 7.2.** *Assume $\mathcal{T}_0$ satisfies Condition B. Let $(\mathcal{T}_k, u_k)$ be the sequence of meshes and solutions produced by the AFEM Algorithm with the modified red-green refinement. Then there exist constants $0 < \xi < 1$, $\beta > 0$, and $C_9 > 0$ such that*

$$e_k^2 + \beta \eta_k^2 \leq C_9 \xi^k. \tag{7.3}$$

*Proof.* The proof of this modified red-green refinement is similar to that of the original red-green refinement.

One main difference is from the proof of Lemma 4.2 and Lemma 6.2. The key of proving Lemma 4.2 is the relation (4.6). From Figure 6, it is easy to find from case (c) and case (e) that a blue element in $\mathcal{T}_k$ may become a red element in $\mathcal{T}_{k+1}$ without any splitting after refinement. Hence, it is necessary to give a new definition of the element-size of blue elements, i.e., the element-size of blue element should be larger than the red element after refinement which in fact without any splitting. On the other hand, a green element may be split into two blue elements after refinement. Therefore, the element-size of blue element should be smaller than the father(green element). In order to keep the relation (4.6) hold, we modify the definition of the blue element-size as (7.2). In fact, $\kappa$ occurred in (7.2) can be any constant in the interval $(1, 2)$. Based on this modified definition, one can proof Lemma 4.2 in a similar routine. Similarly, Lemma 6.2 will be shown easily using this modified definition.

The other main difference is from the proof of quasi-orthogonality in Lemma 5.1. With this refinement strategy, the possible non-nesting mesh can happen in the following situations: (d), (f), (g) of Algorithm 2, and the local adjusting in Figure 5. The situations of, (d), (f), and the local adjusting in Figure 5, can be proved by proceeding along the same line of Lemma 5.1. But we only need a much weaker condition on the initial mesh, namely Condition B since the green refinement is to connect the midpoint of $e_B$ and its opposite vertex. To see this, the readers only need to refer the last inequality of the proof of Lemma 5.1 where we use the relation between the length of the edge and the area of

the coarser element $K$. For the situation (g), we take Figure 4 as example. There are two cases in this situation: (1) the hanging node lies on the boundary $\overline{P_2P_3}$ of the element $T_3$; (2) the hanging node lies on the boundary $\overline{P_1P_4}$ or $\overline{P_3P_4}$ of the element $T_2$. The proof of the case (2) is the same as those for the cases (d) and (f); the case (1) will be locally adjusted as shown in Figure 6 which actually generates the local nested mesh. □

## 8. Conclusion

In this paper, we prove the convergence of AFEM algorithm with the red-green refinement under Condition A. With this result, we conclude that the AFEM algorithm converges for the case where the initial mesh is "good" in the sense of Remark 2.2. In addition, we show the convergence of AFEM algorithm with the modified red-green refinement under Condition B. The discussion in Remark 7.1 indicates that Condition B is actually satisfied by almost all practical meshes. In fact, the often used Delaunay triangulation generates the equilateral triangles in the interior of the domain. Therefore, we only need to use the modified red-green refinement in a layer near the boundary of the domain where the Condition A may fail.

## References


[1] M. Ainsworth and J. T. Oden, *A posteriori error estimation in finite element analysis*, Pure and Applied Mathematics. Wiley-Interscience. John Wiley Sons, New York (2000).

[2] I. Babuska and W. C. Rheinboldt, Error estimates for adaptive finite element computations, SIAM J. Numer. Anal. 15, (1978) 736-754.

[3] R. E. Bank, A. H. Sherman and A. Weiser, Refinement Algorithms and Data Structures for Regular Local Mesh Refinement, Scientific Computing (Applications of Mathematics and Computing to the Physical Sciences) (R. S. Stepleman, ed.), North-Holland (1983) 3-17.

[4] R. E. Bank, The efficient implementation of local mesh refinement algorithms, Adaptive Computational Methods For Partial Differential Equations(I. Babuska, J. Chandra, J. E. Flaherty; eds.), SIAM, Philadelphia, (1983).

[5] R. Becker, S. Mao, An optimally convergent adaptive mixed finite element method, Numer. Math., 111 (2008), 35-54.

[6] S. C. Brenner and L. R. Scott, *The Mathematical Theory of Finite Element Methods*, Springer Verlag, 2nd Edition (2002).

[7] F. Brezzi and M. Fortin, *Mixed and Hybrid Finite Element Methods*, Springer, Berlin, (1991).

[8] C. Carstensen and R. H. W. Hoppe, Error reduction and convergence for an adaptive mixed finite element method, Math. Comp. 75, (2006) 1033-1042.

[9] C. Carstensen and R. H. W. Hoppe, Convergence analysis of an adaptive nonconforming finite element methods, Numer. Math. 103, (2006) 251-266.

[10] J. M. Cascon, Ch. Kreuzer, R. H. Nochetto and K. G. Siebert, Quasi-optimal convergence rate for an adaptive finite element method, SIAM J. NUMER. Anal. 46, (2008) 2524-2550.

[11] J. Cervenka, URL: http://www.iue.tuwien.ac.at/phd/cervenka/node14.html

[12] L. Chen, M. J. Holst, and J. C. Xu, Convergence and optimality of adaptive mixed finite element methods, Math. Comp. 78, (2009) 35–53.

[13] P. G. Ciarlet, *The Finite Element method for Elliptic Problwms*, Amsterdam, North-Holland (1978).

[14] W. Dörfler, A convergent adaptive algorithm for Poisson's equation., SIAM J. Numer. Anal. 33, (1996) 1106-1124.

[15] P. Fleischmann, URL: http://www.iue.tuwien.ac.at/phd/fleischmann/node23.html

[16] J. Hu, Z. C. Shi and J. C. Xu, The convergence of the adaptive Morley-type elements, Preprint, 2009.

[17] J. Hu and J. C. Xu, Convergence of adaptive conforming and nonconforming finite methods for the perturbed stokes equation, preprint, (2008).

[18] E. Leitner and S. Selberherr, Three-Dimensional Grid Adaptation Using a Mixed-Element Decomposition Method, Simulation of Semiconductor Devices and Processes,(H. Ryssel and P. Pichler; eds), Springer, Wien, Austria, 6(1995) 464-467.

[19] K. Mekchay and R. H. Nochetto, Convergence of adaptive finite element methods for general second order linear elliptic PDE, SIAM J. Numer. Anal. 43, (2005) 1803-1827.
[20] N. Molino, R. Bridson, J. Teran and R. Fedkiw, "A Crystalline, Red Green Strategy for Meshing Highly Deformable Objects with tetrahedra," In 12th International Meshing Roundtable, Sandia National Laboratories, (2003) 103-114.
[21] P. Morin, R. H. Nochetto and K. G. Siebert, Data oscillation and convergence of adaptive FEM, SIAM J. Numer. Anal. 38, (2000) 466-488.
[22] P. Morin, R. H. Nochetto and K. G. Siebert, Convergence of adaptive finite element methods, SIAM Review 44, (2002) 631-658.
[23] R. Stevenson, Optimality of a standard adaptive finite element method, Foundations of Computational Mathematics 7, no. 2, (2007) 245-269.
[24] R. Stevenson, The completion of locally refined simplicial partitions created by bisection, Tech. Report, Department of Mathematics, Utrecht University, (2006).
[25] A. Taakili and R. Becker, URL: http://web.univ-pau.fr/~becker/ConchaBase/ConchaBasePool/RedGreen/
[26] R. Verfürth, *A review of a posteriori error estimation and adaptive mesh-refinement techniques*, Wiley-Teubner, Chichester (1996).

Institute of Computational Mathematics, Academy of Mathematics and Systems Science, Chinese Academy of Sciences, Beijing 100190, P. R. China.
*E-mail address*: zhaoxy@lsec.cc.ac.cn

LMAM and School of Mathematical Sciences, Peking University, Beijing 100871, P. R. China.
*E-mail address*: hujun@math.pku.edu.cn

Institute of Computational Mathematics, Academy of Mathematics and Systems Science, Chinese Academy of Sciences, Beijing 100190, P. R. China.
*E-mail address*: shi@lsec.cc.ac.cn